

*On leave of absence from Central Research Laboratory, Texas Instruments Inc., Dallas, Tex. 75222.

¹R. A. Hewes and J. F. Sarver, *Phys. Rev.* **182**, 427 (1969).

²J. E. Geusic, F. W. Ostermayer, H. M. Marcos, L. G. Van Uitert, and J. P. van der Ziel, *J. Appl. Phys.* **42**, 1958 (1971).

³J. D. Kingsley, *J. Appl. Phys.* **41**, 175 (1970).

⁴R. K. Watts, *J. Chem. Phys.* **53**, 3552 (1970).

⁵M. J. Weber, *Phys. Rev. B* **4**, 2932 (1971).

⁶Texas Instruments type TIXL 16, fall time 0.2 μ sec.

⁷Th. Förster, *Ann. Physik* **2**, 55 (1948).

⁸D. L. Dexter, *J. Chem. Phys.* **21**, 836 (1953).

⁹M. Inokuti and F. Hirayama, *J. Chem. Phys.* **43**, 1978 (1965).

¹⁰R. Orbach, in *Optical Properties of Ions in Crystals*,

edited by H. M. Crosswhite and H. W. Moos (Interscience, New York, 1967), p. 445.

¹¹M. Yokota and O. Tanimoto, *J. Phys. Soc. Japan* **22**, 779 (1967).

¹²L. A. Riseberg and H. W. Moos, *Phys. Rev.* **174**, 429 (1968).

¹³H. E. Rast, H. H. Caspers, and S. A. Miller, *Phys. Rev.* **180**, 890 (1969).

¹⁴E. Nakazawa and S. Shionoya, *J. Chem. Phys.* **47**, 3211 (1967).

¹⁵F. W. Ostermayer, Jr., J. P. van der Ziel, H. M. Marcos, L. G. Van Uitert, and J. E. Geusic, *Phys. Rev. B* **3**, 2698 (1971).

¹⁶W. B. Gandrud and H. W. Moos, *J. Chem. Phys.* **49**, 2170 (1968).

Crystal Dynamics of Magnesium Oxide

R. K. Singh and K. S. Upadhyaya

Department of Physics, Banaras Hindu University, Varanasi-5, India

(Received 4 October 1971)

The crystal dynamics of magnesium oxide have been studied by incorporating the effect of three-body interactions in the framework of the shell model on the lines of the work of Singh and Verma [*Phys. Rev. B* **2**, 4288 (1970)]. The theoretical dispersion curves in the three symmetry directions and specific-heat variation with temperature have been calculated and compared with the corresponding experimental results. The experimentally observed second-order infrared absorption and the Raman spectra have also been interpreted by using the critical-point analysis and the combined-density-of-states approach. An excellent agreement has been obtained with the recently measured neutron-scattering, specific-heat, and second-order infrared-absorption and Raman-scattering data.

I. INTRODUCTION

In recent years, the availability of the phonon dispersion relations for magnesium oxide by means of the inelastic scattering of thermal neutrons has stimulated considerable interest in the study of its lattice dynamics among both theoretical and experimental workers. It is a solid of great interest and crystallizes in sodium-chloride structure. The studies of the lattice energy and other properties made by Huggins and Sakamoto¹ clearly show that it is purely an ionic solid and its ions Mg and O possess two units of charges (i. e., Mg²⁺ and O²⁻). This material has been found to exhibit a very large deviation from the Cauchy relation ($C_{12} = C_{44}$), C_{44} being approximately twice as large as C_{12} . It has also been observed that the polarizability of the Mg²⁺ is negligibly small as compared to that of O²⁻. Obviously, for a complete investigation of the physical properties of MgO one must use a lattice-dynamical model capable of describing both the elastic and dielectric behavior of ionic solids.

The pioneering work of Kellermann^{2,3} on the dynamics of crystal lattices with NaCl struc-

ture explains the average properties like specific heat well but presents a very poor description of the details of the vibration spectra. The limitations of the theory can be traced to two simplifying assumptions: (a) The ions of the solid are rigid spheres and (b) they interact through central two-body interactions. These assumptions directly lead to the Cauchy relation ($C_{12} = C_{44}$) and fix the value of the high-frequency dielectric constant as unity. Experiments, however, do not support either of these two results, and one is led to believe that the assumptions impose too strong restrictions on the motion of the ions, particularly the outer electronic shells (unpolarizable ions). Thus the rigid-ion model does not take into account the electronic polarization and hence does not include the effect of distortions of the ions due to the lattice waves. A simple presentation of the electronic polarization and distortion effects in ionic crystals is given by an elegant phenomenological theory, which is known as the shell model and has been introduced by Dick and Overhauser⁴ and Hanlon and Lawson.⁵ This model, extended by Woods, Cochran, and Brockhouse⁶ and by Cochran,^{7,8} considers the ions to be

divided into two parts: (i) a rigid shell of outer electrons and (ii) a rigid core comprising the nucleus and the remaining (inner) electrons. The model has been found to present an excellent description of the dielectric properties of the ionic crystals and has been very popular in recent years. However, it does not go beyond the rigid-ion model in respect of the elastic properties. The main cause of this drawback seems to be the assumption of rigid electronic shells, which is the reason why a number of models have been developed by ascribing some kind of deformation of the shells (Nüsslein and Schröder,^{9,10} Karo and Hardy,¹¹ Melvin *et al.*,¹² and Basu and Sengupta¹³). These models have been found to be very successful, but most of them have been developed by introducing artificial constraints consisting of noncentral forces into the framework of the rigid-shell model of Woods *et al.*⁶

Recently, a modified shell model has been developed by Verma and Singh¹⁴ (see also Singh and Verma¹⁵⁻¹⁸ and Singh¹⁹) which takes account of the deformation effects of electron shells by introducing the matrix elements of the three-body overlap forces within the framework of the shell model of Woods *et al.*⁶ The model has achieved great success in describing the elastic and dielectric properties of the lighter¹⁴⁻¹⁹ as well as heavier alkali halides (Lal and Verma²⁰). The modifications introduced in the shell model by these authors seem to be quite realistic and get strong support from the shell model derived by Sinha^{21,22} from quantum-mechanical considerations. The identical equations obtained by Sinha also indicate the fact that Verma and Singh's modified shell model is not simply a phenomenological model but has a fundamental basis. These considerations together with the successful results obtained in the case of alkali halides¹⁴⁻²⁰ show that the model promises to give a satisfactory description of lattice dynamics of all the ionic solids.

The main aim of the present work is to investigate how well the model of Verma and Singh can describe the lattice dynamics of MgO, which is an important member of another class of ionic solids. The model has been investigated for MgO, for which it is quite reasonable to ignore the polarizability of the positive ions ($\alpha_1 = 0.094 \text{ \AA}^3$ and $\alpha_2 = 3.88 \text{ \AA}^3$; see Peckham²³). This leads to the neglect of the mechanical polarization of these ions, and therefore the basic equations of the model used here are slightly different from Verma and Singh's model. The results reported in this paper for the phonon dispersion relations show an excellent agreement with the experimental neutron-scattering results of Sangster *et al.*²⁴ The definite improvement obtained over the simple shell model indicates the importance of the inclusion of three-body interactions. The frequency shifts in the second-

order Raman-scattering and infrared-absorption spectra computed by using the critical-point analysis (Burstein *et al.*,^{25,26} and Loudon²⁷) and the combined-density-of-states approach (Smart *et al.*²⁸) have been found to present a much better interpretation of the experimental data available. The Debye characteristic temperature Θ_D computed as a function of temperature T has also been found to give a fairly good agreement with experimental data of Barron *et al.*²⁹

In Sec. II we give a brief description of the exact form of Verma and Singh's model used here. The results obtained are given in Sec. III and they are discussed in Sec. IV.

II. MODIFIED SHELL MODEL FOR MgO

The present model for the lattice dynamics of MgO follows almost identically the modified shell model described in detail by Singh and Verma¹⁷ and reviewed by Cochran.³⁰ The number of parameters has been reduced by making the following assumptions: (i) The ionic charge Ze is $2e$; (ii) only the oxygen ions are polarizable; and (iii) the short-range forces act between (a) the nearest-neighbor shells and (b) the shells and their own cores of the ions. Since we consider only one ion to be polarizable and deformable, the basic equations of Singh and Verma's model are modified in the following form:

$$\begin{aligned} M\omega^2 \vec{U} &= (\underline{R} + \underline{Z} \underline{C}' \underline{Z}) \vec{U} + (\underline{R} + \underline{Z} \underline{C}' \underline{Y}) \vec{W}, \\ 0 &= (\underline{R} + \underline{Y} \underline{C}' \underline{Z}) \vec{U} + (\underline{R} + \underline{K} + \underline{Y} \underline{C}' \underline{Y}) \vec{W}, \end{aligned} \quad (1)$$

where, as in the usual shell model, \vec{U} and \vec{W} stand for the core displacement vector and the displacement vector of the shells relative to their own cores, respectively. \underline{M} , \underline{Z} , \underline{Y} , and \underline{K} are the 6×6 diagonal matrices defined as in the case of the one-ion-polarizable shell model. Their elements are formed, respectively, from the ion masses, ion charges, shell charges, and shell-core force constants. \underline{R} is the short-range interaction matrix representing the shell-shell interactions between the nearest neighbors as given by Woods *et al.*,⁶ and \underline{C}' is the long-range interaction matrix defined by Singh and Verma,¹⁷ which specifies the interactions arising from the electrostatic forces and the shell deformations (three-body overlap forces).

By solving Eq. (1) in the long-wavelength limit we obtain the following expressions for the elastic constants (C_{11} , C_{12} , C_{44}) and the optical vibration frequencies (ν_L , ν_T) in terms of the model parameters:

$$2r_0 C_{11} = \frac{(Ze)^2}{v} \left[A - 5.112 \left(1 + \frac{12}{Z} f(r) \right) + 9.3204 \left(\frac{r}{Z} \frac{df}{dr} \right) \right]_0,$$

$$2r_0 C_{12} = \frac{(Ze)^2}{v} \left[-B + 0.226 \left(1 + \frac{12}{Z} f(r) \right) + 9.3204 \left(\frac{r}{Z} \frac{df}{dr} \right) \right]_0, \quad (2)$$

$$2r_0 C_{44} = \frac{(Ze)^2}{v} \left[B + 2.556 \left(1 + \frac{12}{Z} f(r) \right) \right]_0, \quad (3)$$

$$4\pi^2 \mu \nu_L^2 = R_0 - \frac{e^2 d^2}{\alpha} + \frac{8\pi}{3} \frac{(Z'e)^2}{v f_L} \times \left[\left(1 + \frac{12}{Z} f(r) \right) + 6 \left(\frac{r}{Z} \frac{df}{dr} \right) \right]_0,$$

$$4\pi^2 \mu \nu_T^2 = R_0 - \frac{e^2 d^2}{\alpha} - \frac{4\pi}{3} \frac{(Z'e)^2}{v f_T} \left(1 + \frac{12}{Z} f(r) \right)_0,$$

where Ze represents the ionic charge, r_0 is the equilibrium separation of the nearest neighbors, $v (= 2r_0^3)$ is the volume of the unit cell, the subscript zero on the brackets indicates the equilibrium values of the quantities inside, μ is the reduced mass of the two ions in the unit cell, $f(r)$ is the function dependent on overlap integrals of the electron wave functions defined by Löwdin,³¹ and A and B are the short-range force constants defined by Kellermann.² The remaining symbols have their usual meaning¹⁷:

$$Z' = Z - d, \quad (4)$$

$$R_0 = \frac{(Ze)^2}{v} (A + 2B), \quad (5)$$

$$f_L = 1 + \frac{\alpha}{v} \frac{8\pi}{3} \left[\left(1 + \frac{12}{Z} f(r) \right) + 6 \left(\frac{r}{Z} \frac{df}{dr} \right) \right]_0, \quad (6)$$

$$f_T = 1 - \frac{\alpha}{v} \frac{4\pi}{3} \left(1 + \frac{12}{Z} f(r) \right)_0. \quad (7)$$

The electrical and mechanical polarizabilities (α , d) of the negative ions are given by

$$\alpha = \frac{(Ye)^2}{R_0 + K} = \frac{3v}{4\pi} \left(\frac{\epsilon_\infty - 1}{\epsilon_\infty + 2} \right), \quad (8)$$

$$d = \frac{R_0 Y}{R_0 + K} = -\frac{\alpha R_0}{e^2 Y}. \quad (9)$$

If we choose $Z = 2$ and use the equilibrium condition

$$B = -1.165 \left(1 + \frac{12}{Z} f(r) \right)_0, \quad (10)$$

the remaining five parameters A , $f(r_0)$, $(rdf/dr)_0$, d , and Y can be determined from Eqs. (2)–(9), which give just five independent equations. Once the parameters of the model are known, Eq. (1) can be solved for the vibrational frequencies ν corresponding to each phonon wave vector \vec{q} .

III. NUMERICAL COMPUTATIONS

In the present study the dynamics of crystal lattices of MgO have been investigated in detail by

using the model described in Sec. II and developed by Verma and Singh.¹⁴ The model contains seven parameters: the two short-range force constants A and B , the two parameters $f(r_0)$ and $(rdf/dr)_0$ arising from the deformation forces (three-body overlap forces), the ionic charge Z , the shell charge Y , and the mechanical polarizability d for the O^{2-} ion. These parameters have been calculated by using the neutron data,³³ together with the elastic constants³² and high-frequency dielectric constants³⁵ given in Table I along with the relevant references. The calculated model parameters are also given in Table I.

Now Eq. (1) can be solved to obtain the vibration spectra of MgO for the 48 nonequivalent wave vectors of the first Brillouin zone corresponding to a division in 1000 equal parts by using the parameters listed in Table I. The calculated dispersion relation for phonons propagating along the $(q, 0, 0)$, $(q, q, 0)$, and (q, q, q) directions are shown in Fig. 1, plotted together with the neutron dispersion relations measured by Sangster *et al.*²⁴ The theoretical results obtained by the simple shell model²³ are also included in the figure for visual comparison.

In order to study the dynamical properties like specific heat and second-order infrared-absorption and Raman-scattering data, we have used the computed vibration spectra of MgO. The specific heat and the associated Debye temperatures Θ_D in the harmonic approximation have been calculated as a function of temperature T from the lattice frequency spectra. The comparison of the calculated with that obtained from calorimetric measurements by Barron, Berg, and Morrison²⁹ is shown in Fig. 2.

The combined-density-of-states (CDS) curves have been obtained by computing the density of states $N(\nu_1 + \nu_2)$ of the combination frequencies $(\nu_1 + \nu_2)$ from the knowledge of lattice vibration fre-

TABLE I. Input data and the model parameters of MgO.

	Experimental data		Model parameters		
	Constants	Values	Refs.	Parameters	Values
C_{11} (10^{11} dyn cm^{-2})		28.917	Chung ^a	A	8.003
C_{12} (10^{11} dyn cm^{-2})		8.796	Chung ^a	B	-1.105
C_{44} (10^{11} dyn cm^{-2})		15.461	Chung ^a	$f(r_0)$	-0.009
ν_L (10^{12} sec^{-1})		21.679 ^b	Sangster ^c	$(rdf/dr)_0$	-0.122
ν_T (10^{12} sec^{-1})		11.870	Sangster ^c	Y	-3.205
r_0 (10^{-8} cm)		2.106	Skinner ^d	d	0.681
ϵ_∞		2.957	Stephens and Malitson ^e	Z	2.000

^aReference 32.

^bValue calculated from Lyddane-Sachs-Teller relation (Ref. 36) using $\epsilon_0 = 9.86$ (Sangster *et al.*, Ref. 24).

^cReference 33.

^dReference 34.

^eReference 35.

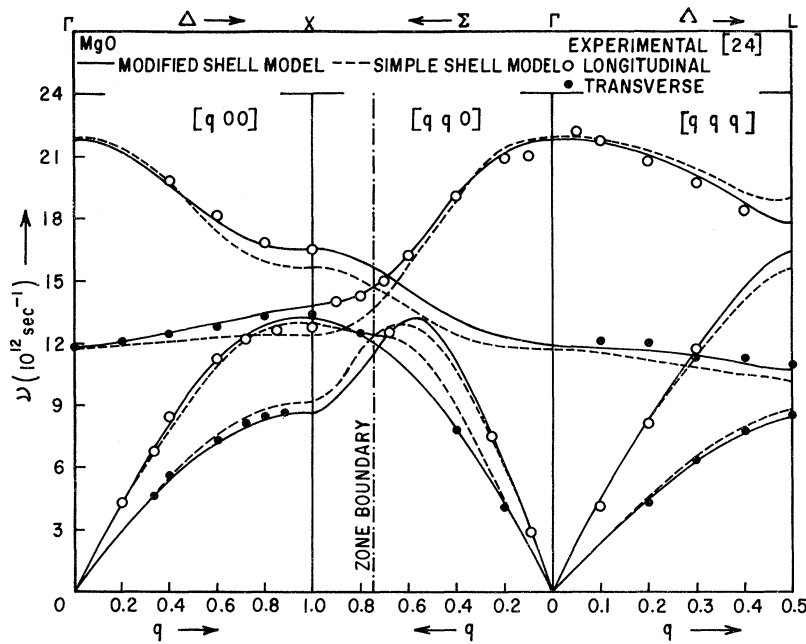


FIG. 1. Phonon dispersion curves for MgO. Full curve, modified shell model (Singh and Verma, Ref. 17); broken curve, simple shell model (Peckham, Ref. 23). The points with open and closed circles, corresponding to the longitudinal and transverse branches, respectively, are experimental (Ref. 24).

quency spectra. The peaks obtained in the CDS curve which correspond to the subsidiary maxima in the two-phonon Raman and infrared (ir) spectra^{37,38} have been compared with experimentally determined peaks and are shown in Fig. 3. The values of the

frequencies corresponding to theoretical and experimental peaks are listed in Table II.

In view of the fact that the two-phonon combination and overtones are Raman active while the latter are infrared inactive in the rocksalt struc-

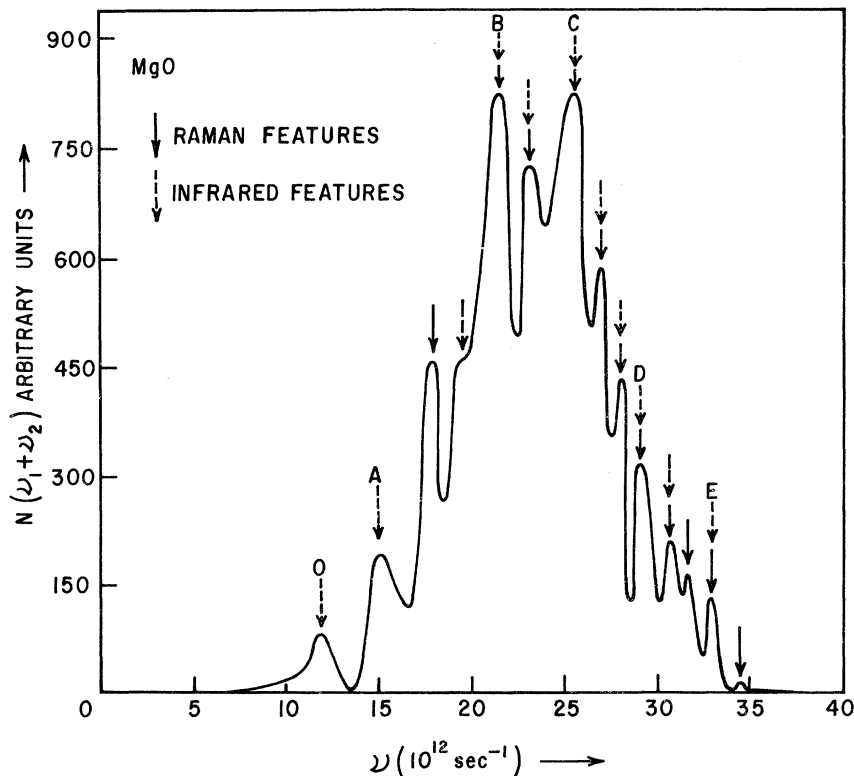


FIG. 2. Debye characteristic temperatures as a function of temperature for MgO. The full curve is derived from vibration spectra (present study); the broken curve from the specific-heat measurements by Barron *et al.* (Ref. 29).

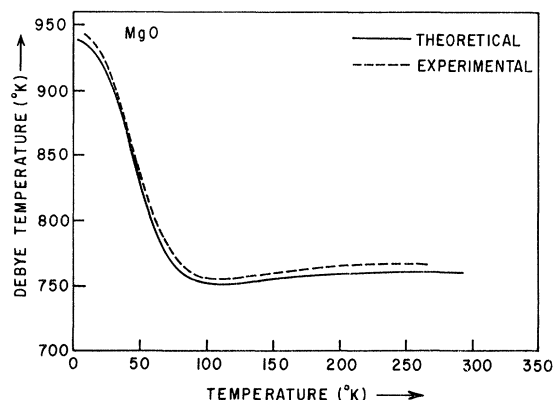


FIG. 3. Combined-density-of-states curve for MgO. The arrows full and broken indicate the positions of observed peaks in Raman-scattering and ir-absorption spectrum, respectively. Assignments O, A, B, C, D, and E specify the positions of the more pronounced absorption peaks.

ture, the exclusion of the two-phonon overtones in the above approach thus leads to an incomplete description of the Raman-scattering data. In order to present a complete interpretation of Raman spectra we have, therefore, used the critical-point analysis,²⁵⁻²⁷ which takes account of both the two-phonon combination and overtones corresponding to the critical points in the Brillouin zone. The computed Raman shifts in terms of overtones and combinations of frequencies corresponding to the critical points (Γ , X , L) in the symmetry directions and compared with those of Manson *et al.*³⁹ calculated from the neutron data²⁴ are shown in Table III. The frequency shifts in ir spectra computed in terms of combinations of frequencies corresponding to the critical points (L , Δ) and compared with those of Martin and David⁴¹ obtained from the simple shell model are also shown in Table III.

IV. DISCUSSION

A glance at the various properties investigated in the present study clearly shows that the Verma and Singh's model provides a completely satisfactory description of lattice dynamics of MgO. It is clear from Fig. 2 that our theoretically computed dispersion relations connecting the frequency of the normal mode of vibration of the crystal lattice to its wave vector agree extremely well with those deduced from the neutron-scattering technique by Sangster *et al.*²⁴ A similar agreement has been obtained by Sangster *et al.*,²⁴ with the help of a nine-parameter breathing-shell model. The model parameters determined from the knowledge of phonon dispersion curves give almost correct values of the elastic constants but yield considerably low values of the dielectric constants. This is a re-

flection of the low value of the ionic charge. This reduction in ionic charge will lead to a great reduction in the cohesive energy of the crystal and hence will spoil the agreement between calculated and measured cohesive energy. Also, the improved agreement obtained in the model is subject to the restriction $G_2 \neq K_2$, which has no theoretical justification³⁰ to retain it. Further, the breathing-shell model proposed by Mon⁴² with $G_2 = K_2$ is found to lead to poor agreement with neutron dispersion curves. On the other hand, the seven parameters in the present model have been determined from the experimental data other than the phonon dispersion data it intends to predict. Also, they yield quite reasonable values of the cohesive energy, elastic constants, and dielectric constants. On the basis of these considerations this model can claim to be relatively more realistic to describe the dielectric and dynamical behavior of MgO.

The theoretical $\Theta_D - T$ curve presented in Fig. 2 shows an excellent agreement with the experimental curve obtained by Barron *et al.*²⁹ The small deviations obtained at higher temperatures are expected because the present model is subject to the harmonic approximation.

A brief inspection of Fig. 3 shows that the peaks of the CDS curves compare favorably with the corresponding peaks observed in the two-phonon Raman

TABLE II. Comparison of observed peaks in fine structure of second-order ir-absorption and Raman-scattering spectrum with calculated CDS peaks for MgO.

Ref. 39 Raman-spectra peaks (observed) (cm^{-1})	Present study CDS peaks (theoretical) (cm^{-1})	Ref. 40 Infrared peaks (observed) (cm^{-1})
...	393	394
...	502	496
592	595	...
...	650	660
712	718	723
742	760	770
801
825
836
858	853	857
870
880	881	880
895	...	891
926	923	921
...	...	958
975	980	982
1019	1020	1012
1048	1052	...
1098	1100	1105
1149	1150	...
...	...	1210
...	...	1380
1470

TABLE III. Assignment of peaks of ir-absorption and Raman-scattering spectra of MgO.

Ref. 39 Neutron- diffraction- data peaks (cm ⁻¹)	Raman active		Ref. 41 Simple- shell-model peaks (cm ⁻¹)	Infrared active	
	Present study	Value (cm ⁻¹)		Present study	Value (cm ⁻¹)
	Assignments			Assignments	
570	2TA(X)	572	570	2TA(Δ)	572
602	630
...	2TO(L)	704	660	TO(L) + TA(L)	656
720	LA(Δ) + TA(Δ)	728
731	LA(X) + TA(X)	728	777	TO(Δ) + TA(Δ)	746
744	TO(X) + TA(X)	745	785
788	2TO(Γ)	792	840	LO(Δ) + TA(Δ)	844
...	LA(L) + TA(L)	832	885	LO(L) + TA(L)	884
855	LO(X) + TA(X)	844	...	TO(L) + LA(L)	898
860	2LA(X)	864	...	TO(Δ) + LA(Δ)	902
873	935	2TO(Δ)	920
876	995	LO(Δ) + LA(Δ)	996
886	TO(X) + LA(X)	902	...	LO(Δ) + TO(Δ)	1014
...	2TO(X)	920	1090	2LO(Δ)	1108
969	LO(L) + TO(L)	950	...	LO(L) + LA(L)	1144
984	1400
997	LO(X) + LA(X)	996			
1032	LO(X) + TO(X)	1014			
1108	2LO(X)	1108			
1114			
...	2LO(L)	1196			
1368			
1440	2LO(Γ)	1446			

and infrared spectra. The comparative results presented in Table II show that the relatively fewer peaks found in the CDS curves are not sufficient to interpret satisfactorily the fine structure of ir absorption and Raman spectra. This limitation can be ascribed to the coarseness of our selection of wave vectors within the Brillouin zone. It is hoped that the model will present a much better description by using more sophisticated ways of computing second-order densities of states relating to the ir-absorption and Raman-scattering spectra. However, Table IV shows that the peaks obtained by us from the CDS curve agree very well with the more pronounced ir-absorption peaks observed by Barnes *et al.*,⁴³ Burstein *et al.*,⁴⁴ and Willmott.⁴⁵ They also all agree with the peaks calculated by Verma and Dayal.⁴⁶ The various peaks observed by different workers⁴⁴⁻⁴⁵ in the ir-absorption spectra generally lie between 8 and 25 μ, which corresponds to the range obtained by us. Further, the computed peak corresponding to the lattice frequency 25.4 μ is in better agreement with the principal peak observed by Saksena and Viswanathan⁴⁷ at 25.26 μ. This shows that the observation of Saksena and Vishwanathan⁴⁷ is reasonably correct and a principal absorption maxima occurs at 25.26 μ. The over-all results of the CDS curve derived from the harmonic theory present sufficiently good

agreement with experiments in view of the spread in the position of the peaks observed by different authors.

It is seen from Tables II and III that the two-phonon Raman and infrared spectra of the solid under consideration find a satisfactory explanation in our scheme. The assignments of Raman spectra obtained by Manson *et al.*³⁹ are very close to those obtained by us. This is expected because our dispersion relations are in exact agreement with neutron data used by them. The basic aim of the detailed study of the two-phonon Raman and ir spectra in the present work is to correlate the

TABLE IV. Comparison of more pronounced CDS and experimental infrared-absorption peaks of MgO.

CDS peaks		Experimental ir-absorption peaks		
Present study	Verma and Dayal ^a	Willmott ^b	Barnes <i>et al.</i> ^c	Burstein <i>et al.</i> ^d
λ (μ)	λ (μ)	λ (μ)	λ (μ)	λ (μ)
25.40	25.0	24.30	...	22.00
19.97	18.1	17.50	15.4	16.00
15.14	15.2	14.80	14.4	...
11.87	12.3	11.70	11.8	11.82
10.18	10.5	10.07	10.2	10.18
9.07	9.1	...	8.8	8.30

^aReference 46.^bReference 45.^cReference 43.^dReference 44.

neutron and optical experimental results on MgO. It is expected that the study will be useful in deducing the values of individual phonon frequencies and in investigating the optical and infrared properties of MgO to explain the considerable coupling between the modes of vibration of its ions.⁴³ In this connection, it would perhaps be worthwhile to mention that the study will prove to be much more important if more sophisticated programs now available for generating density of states functions^{48,49} are used rather than the crude root-sampling method used here.

The results discussed above show that in spite of the successful and satisfactory agreement obtained between theory and experiment there are small discrepancies. These are not unexpected and may be mainly due to the lack of inclusion of anharmonic effects and higher-order neighbor-in-

teraction effects.

ACKNOWLEDGMENTS

The authors wish to express their gratitude to Professor B. Dayal, Department of Physics, Institute of Advance Studies in Sciences, Meerut University, Meerut, and to Dr. M. P. Verma, Department of Physics, Agra College, Agra, for their helpful discussions and encouragement. We are also thankful to Professor M. L. J. Sangster, Department of Physics, University of Reading, England, for communicating the experimental data privately, and to Professor G. S. Verma, Head, Department of Physics, Banaras Hindu University, for providing necessary facilities. One of the authors (KSU) would like to express his gratitude to the Council of Scientific and Industrial Research for the award of a fellowship.

¹M. L. Huggins and Y. J. Sakamoto, J. Phys. Soc. Japan **12**, 241 (1957).

²E. W. Kellermann, Phil. Trans. Roy. Soc. London **A238**, 513 (1940).

³E. W. Kellermann, Proc. Roy. Soc. (London) **A178**, 17 (1941).

⁴B. J. Dick and A. W. Overhauser, Phys. Rev. **112**, 90 (1958).

⁵J. E. Hanlon and A. W. Lawson, Phys. Rev. **113**, 472 (1959).

⁶A. D. B. Woods, W. Cochran, and B. M. Brockhouse Phys. Rev. **119**, 980 (1960).

⁷W. Cochran, Phil. Mag. **4**, 1082 (1959).

⁸W. Cochran, Proc. Roy. Soc. (London) **A253**, 280 (1959).

⁹V. Nüsslein and U. Schröder, Phys. Status Solidi **21**, 309 (1967).

¹⁰U. Schröder, Solid State Commun. **4**, 347 (1966).

¹¹A. M. Karo and J. R. Hardy, Phys. Rev. **129**, 2024 (1963).

¹²J. S. Melvin, J. D. Pirie, and T. Smith, Phys. Rev. **175**, 1082 (1968).

¹³A. N. Basu and S. Sengupta, Phys. Status Solidi **29**, 367 (1968).

¹⁴M. P. Verma and R. K. Singh, Phys. Status Solidi **33**, 769 (1969).

¹⁵R. K. Singh and M. P. Verma, Phys. Status Solidi **36**, 335 (1969).

¹⁶R. K. Singh and M. P. Verma, Phys. Status Solidi **38**, 851 (1970).

¹⁷R. K. Singh and M. P. Verma, Phys. Rev. B **2**, 4288 (1970).

¹⁸M. P. Verma and R. K. Singh, J. Phys. C **4**, 2745 (1971).

¹⁹R. K. Singh, Ph.D. thesis (Banaras Hindu University, 1969) (unpublished).

²⁰H. H. Lal and M. P. Verma, Indian J. Pure Appl. Phys. **8**, 380 (1970); and private communication.

²¹S. K. Sinha, Phys. Rev. **177**, 1256 (1969).

²²S. K. Sinha, Phys. Rev. **169**, 477 (1968).

²³G. Peckham, Proc. Phys. Soc. (London) **90**, 657 (1967).

²⁴M. L. J. Sangster, G. Peckham, and D. H. Saunderson, J. Phys. C **2**, 1026 (1970).

²⁵E. Burstein, F. A. Johnson, and R. Loudon, Phys. Rev. **139**, A1239 (1965).

²⁶E. Burstein, in *Proceedings of International Conference on Lattice Dynamics, Copenhagen*, 1963, edited by R. F. Wallis (Pergamon, Oxford, 1965), p. 315.

²⁷R. Loudon, Phys. Rev. **137**, A1784 (1965).

²⁸C. Smart, G. R. Wilkinson, A. M. Karo, and J. R. Hardy, Ref. 26, p. 387.

²⁹T. H. K. Barron, W. T. Berg, and J. A. Morrison, Proc. Roy. Soc. (London) **A250**, 70 (1953).

³⁰W. Cochran, CRC Critical Rev. Solid State Sci. **1**, 1 (1971).

³¹P. O. Löwdin, Arkiv. Mat. Astron. Fys. **35A**, 30 (1947).

³²D. H. Chung, Phil. Mag. **8**, 833 (1963).

³³M. L. J. Sangster (private communication).

³⁴B. J. Skinner, Am. Mineralogist **42**, 39 (1957).

³⁵R. E. Stephens and I. H. Malitson, J. Res. Natl. Bur. Std. (U. S.) **49**, 249 (1952).

³⁶R. H. Lyddane, R. G. Sachs, and E. Teller, Phys. Rev. **59**, 673 (1941).

³⁷B. Szigeti, Proc. Roy. Soc. (London) **A252**, 217 (1959).

³⁸B. Szigeti, Proc. Roy. Soc. (London) **A258**, 337 (1960).

³⁹N. B. Manson, W. V. Ohe, and S. L. Chodos, Phys. Rev. B **3**, 1968 (1971).

⁴⁰H. G. Hafele, Ann. Physik **10**, 321 (1963).

⁴¹A. H. Martin and W. J. David, Trans. Faraday Soc. **65**, 2016 (1969).

⁴²J. P. Mon, Phys. Status Solidi **21**, 309 (1969).

⁴³R. B. Barnes, R. Brattain, and F. Seitz, Phys. Rev. **48**, 582 (1935).

⁴⁴E. Burstein, J. J. Oberley, and E. K. Plyler, Proc. Indian Acad. Sci. **28A**, 388 (1948).

⁴⁵J. C. Willmott, Proc. Phys. Soc. (London) **A63**, 389 (1950).

⁴⁶M. P. Verma and B. Dayal, Phys. Status Solidi **19**, 751 (1967).

⁴⁷B. D. Saksena and S. Vishwanathan, Proc. Phys. Soc. (London) **B69**, 129 (1956).

⁴⁸G. Dolling and R. A. Cowley, Proc. Phys. Soc. (London) **88**, 463 (1966).

⁴⁹G. Gilat and L. J. Raubenheimer, Phys. Rev. **144**, 390 (1966).

PHYSICAL REVIEW B

VOLUME 6, NUMBER 4

15 AUGUST 1972

Softening of the Rotary Lattice Mode in K_2PtBr_6 as Detected by Nuclear Quadrupole Resonance*

Henry M. Van Driel,[†] Maria Wiszniewska,[‡]

B. Michael Moores, and Robin L. Armstrong

Department of Physics, University of Toronto, Toronto, Canada

(Received 7 June 1971; revised manuscript received 24 January 1972)

Measurements of the ⁷⁹Br nuclear-quadrupole-resonance frequency and spin-lattice relaxation time in a polycrystalline sample of K_2PtBr_6 from 4 to 450 K are reported. The frequency data indicate that structural phase transitions occur at 78, 105, 137, 143, and 169 K. The relaxation-time data are extremely sensitive to the phase transition at 169 K. At the high-temperature phase transition the structure of the substance changes from cubic to tetragonal. On the basis of previous comprehensive studies in K_2ReCl_6 it is likely that the phase transition is second order and is driven by the rotary lattice mode. As a model for this transition it is assumed that the $PtBr_6^{2-}$ octahedra remain undistorted but that they rotate within the cages defined by neighboring K^+ ions and that the cages elongate in the directions of the axes of rotation of the octahedra. The frequency data in the high-temperature phase are analyzed to yield the temperature dependence of a certain average $\bar{\omega}_v$ of the rotary-lattice-mode frequency over the Brillouin zone; a 12% softening is deduced. The relaxation data in the high-temperature phase are analyzed to yield the temperature dependence of a second average $\bar{\omega}_{T_1}$ of the rotary-mode frequency over the Brillouin zone; a 40% softening is deduced. It is shown that the difference between the temperature dependence of $\bar{\omega}_v$ and $\bar{\omega}_{T_1}$ is due to a difference in weighting of the rotary-mode frequency near the Brillouin-zone center. In particular, the dramatic temperature dependence of $\bar{\omega}_{T_1}$ can only be accounted for through the anharmonic Raman process and not the ordinary Raman process for quadrupolar-dominated spin-lattice relaxation. Below 169 K, two T_1 values, one approximately twice the other, are observed at each temperature. It is shown that this observation is consistent with the model postulated for the phase transition. The average rotary-mode frequency is found to harden as the temperature decreases below 169 K. That T_1 is insensitive to the phase transitions at lower temperatures is thought to imply that these transitions are not driven by the rotary-lattice mode.

I. INTRODUCTION

Nuclear-quadrupole-resonance (NQR) research carried out at the University of Toronto in recent years¹⁻⁵ to study the cubic R_2MX_6 compounds has shown that the temperature and pressure dependences of the resonance frequencies and spin-lattice relaxation rates of chlorine nuclei predominantly reflect the behavior of the low-lying rotary-lattice mode. Because of symmetry considerations this mode is neither infrared nor Raman active in the cubic phase, and therefore, NQR spectroscopy provides an especially attractive technique for the study of the rotary mode.

Many of the R_2MX_6 compounds exhibit multiple phase transitions from their high-temperature cubic phase to lower-symmetry phases as the temperature is decreased. It was suggested by O'Leary⁶ that the temperature variation of pure-NQR-frequency data could be used to advantage for the observation of the softening of low-fre-

quency librational modes in regions otherwise inaccessible to spectroscopic investigation. He presented data for the ³⁵Cl NQR in K_2ReCl_6 and analyzed the data in the region of the crystallographic phase transition at 110.9 K. The analysis of the experimental information for this paramagnetic compound is complicated by the possible contribution from π bonding and by large specific-volume effects.³ To circumvent these difficulties we decided to study the ⁷⁹Br resonance in diamagnetic K_2PtBr_6 in which π bonding is not present and in which specific-volume effects are likely to be considerably less important.

Unfortunately, much less is known about the phase transitions in K_2PtBr_6 than in K_2ReCl_6 . In our analysis we will rely on the results of the comprehensive analysis available for K_2ReCl_6 .⁷ In this salt the phase transition at 110.9 K is thought to be a displacive phase transition of the second kind in the Landau sense. According to the Landau theory the phase transition is brought